# Clarke Transform Based Fast Assessment of Switching Overvoltages in An MV Distribution Network


## Abstract

The paper investigates the use of the Clarke transform in time-domain simulations, namely the evaluation of transient overvoltages in medium voltage (MV) distribution networks. A simplified Clarke equivalent circuit can be set up using readily available symmetrical components data used in steady-state studies, such as line series impedances and the aggregate MV network capacitance. Attention was focused on an existing 20 kV radial distribution system, a large mixed cable/overhead network operated with ungrounded neutral. The worst-case scenario of a single-line-to-ground (1LG) fault occurring at the end of a long overhead line was simulated by means of equivalent lumped-parameter Clarke circuits which were implemented and solved by means of ATP-EMTP [44]. An extensive transient simulation parametric study was carried out using Clarke circuits with different degrees of simplification, and results were compared with those yielded by a complete 3-phase ATP model, evidencing a very good agreement and a drastic reduction of computation times.



Index Terms— Clarke Transform, Fault current, Power distribution faults, Power system transients, Transient Overvoltages


## 1 Introduction

The theory of symmetrical components [1] allows a significant simplification of the steady-state analysis of symmetrical three-phase networks in case of unbalanced faults. The faulted three-phase network, with mutual couplings between the three phases, is replaced by three symmetrical, uncoupled sequence networks connected only at the fault location, greatly reducing the required calculations.

After Fortescue several other circuit transformations have been subsequently proposed: e.g. by Clarke [2][3], Kimbark and Boyajyan [4], Koga [5], Rama Rao [6]. Each of these coordinate's systems are defined by its own transformation matrix and may be regarded as a particular solution to the

eigenvalue problem, i.e., the diagonalization of the network's impedance matrix. In stark contrast to the widespread use of Fortescue's symmetrical components, later transformations see little use today.

Since the 1930s there have also been attempts to extend the advantages of symmetrical components from phasors to time-domain quantities, thus decoupling not only the fundamental but every oscillation frequency of the circuit response into single-phase, separated quantities which do not interact between each other.

Various papers discussed the extension of symmetrical components to transient calculations [7][8], and there are examples of their application to practical case studies, such as transient recovery voltages [9] [10][11] or travelling waves analysis on transmission lines [12][13]. All these papers were limited to analytical treatment. On the other hand, employing numerical (computer) circuit simulation to eventually solve the sequence networks in the time domain is hardly feasible because, once the sequence networks has been resolved, the computation of phase voltages and currents back from the sequence quantities would require the multiplication of the latter by the complex operators $a = e^{j\,2/3\pi}$ and $a^2 = e^{j\,4/3\pi}$. This precludes the applicability of symmetrical components in transient calculations when the network has more than a few buses.

If the network is solved analytically, so that an expression for all the sequence quantities is available in operational form (as a steady-state sinusoidal term plus a number of exponentially decaying terms [14]), then the aforementioned multiplications can be accomplished by separately applying the operators to each component. On the contrary, if the sequence quantities are available simply as an array of numerical values (as is the case if circuit simulation software is employed), apart from a few special cases there is no way to get the phase quantities back from sequence quantities [15].

This problem can be overcome by using a transform defined by a real-valued transformation matrix, such as the Clarke transform [16]. Its 0, α and β components are well suited for manipulating time-domain quantities, either analytically [17][18] or via numerical calculation. Today, the Clarke transform (and related concepts, such as Park transform and space vectors) finds a wide spectrum of applications:

- induction machine analysis [19] and AC-DC converter theory [20][21]. In [22], the classical theory is extended from electrical machines to the entire three-phase power systems by using the space vector approach,
- power quality [23],
- modal analysis [24],
- transformer protection [25].

Recently, there has been some renewed interest in the application of the Clarke transform to system transients, such as short circuits, open-circuit faults and transient recovery voltages [26] - [32]. In [33] a simplified method to estimate peak short circuit currents in networks of arbitrary topology is proposed. In all cited papers, the focus is generally on the applicability of the Clarke transform to the solution of power system transients, from a theoretical point of view, by defining the equivalence between a generic three-phase network, composed by a Thévenin equivalent and a load, and its corresponding Clarke representation.

The present paper specifically deals with the application of the method to large-sized systems, namely the time-domain simulations of fault transients in large, real life distribution network by means of Clarke equivalents. The purpose of the study is to show the applicability of a Clarke-based approach to transient simulation of realistic MV systems; the accuracy of results and the computation time savings are checked by comparison with standard EMTP-type simulation models.

The paper thus reports an extensive time-domain parametric study of single-line-to-ground (1LG) faults in a radial medium voltage (MV) distribution networks, aimed at assessing the overvoltages' envelope. It is known that following a 1LG fault, a network operated with ungrounded neutral can incur in very severe overvoltages [35][36][37], both transient and temporary. In [35], [36] it was shown that temporary overvoltages up to 3.5 p.u. can develop on the healthy phases of a radial MV network characterized by a large aggregate zero-sequence capacitance, when a 1LG fault occurs at the receiving end of a long radial overhead line. The temporary overvoltage is normally higher at the HV/MV substation busbars, due to zero-sequence reactive power flowing towards the fault. This was

experimentally verified by means of staged faults in a real MV distribution network [36] which yielded the predicted TOVs, up to 2.25 pu; transient overvoltages were even larger. Should the insulation on either of the healthy phases fail, a Cross-Country fault would occur [36].

In this paper, the study is performed by means of simplified, lumped-parameters equivalent circuits, derived from the application of the Clarke transform and solved in ATP. The steady-state as well as the transient response of the network following the 1LG fault is decoupled into three separated components, each of which is associated to a single-phase equivalent network (namely, 0, α and β component networks), connected to each other only at fault location. Various type of Clarke equivalent circuits, characterized by different degrees of approximation, are set up and the waveforms obtained from the simulations are systematically compared with those yielded by a complete ATP three-phase network model, taken as a benchmark. The effects of different parameters (e.g., fault resistance, fault inception time or fault location along the feeder) on the accuracy of the model are outlined. The drastic saving in computation time is also quantified.

The paper is organized as follows: Section 2 presents a summary of the Clarke transformation and its application to time-domain studies. Section 3 focuses on the 1LG fault approach using Clarke's 0, α and β component networks. Sections 4 and 5 describe the application of the method to two different case studies.

## 2 Clarke components

In this paper, a slightly modified version of the original Clarke transform [2] is used [34]. It is based on an orthogonal transformation matrix, so the connection of component networks to represent system unbalances can be done by means of coupling transformers. Phase voltages are related to their (0, α, β) components as follows:

$$\begin{pmatrix} v_a \\ v_b \\ v_c \end{pmatrix} = \begin{pmatrix} \frac{1}{\sqrt{3}} & \frac{\sqrt{2}}{\sqrt{3}} & 0 \\ \frac{1}{\sqrt{3}} & \frac{-1}{\sqrt{6}} & \frac{1}{\sqrt{2}} \\ \frac{1}{\sqrt{3}} & \frac{-1}{\sqrt{6}} & \frac{-1}{\sqrt{2}} \end{pmatrix} \cdot \begin{pmatrix} v_0 \\ v_\alpha \\ v_\beta \end{pmatrix} \qquad (1)$$

A similar equation holds for currents.

The systematic substitution of the voltages and currents of the three-phase network with the new components defined by (1) leads in turn to the definition of the attendant 0, α and β component networks. Let us consider a generic three-phase, static, symmetrical element (i.e., a coupled RLC circuit) connecting buses S and R of the three-phase network, described in time-domain by the following general set of equations:

$$\begin{pmatrix} v_{as} \\ v_{bs} \\ v_{cs} \end{pmatrix} - \begin{pmatrix} v_{aR} \\ v_{bR} \\ v_{cR} \end{pmatrix} = \begin{pmatrix} \Delta v_a \\ \Delta v_b \\ \Delta v_c \end{pmatrix} = \overbrace{\begin{pmatrix} R_p & R_m & R_m \\ R_m & R_p & R_m \\ R_m & R_m & R_p \end{pmatrix}}^{R} \cdot \begin{pmatrix} i_a \\ i_b \\ i_c \end{pmatrix} + \overbrace{\begin{pmatrix} L_p & L_m & L_m \\ L_m & L_p & L_m \\ L_m & L_m & L_p \end{pmatrix}}^{L} \cdot \begin{pmatrix} \frac{di_a}{dt} \\ \frac{di_b}{dt} \\ \frac{di_c}{dt} \end{pmatrix} + \overbrace{\begin{pmatrix} S_p & S_m & S_m \\ S_m & S_p & S_m \\ S_m & S_m & S_p \end{pmatrix}}^{S} \cdot \int_{-\infty}^{t} \begin{pmatrix} i_a \\ i_b \\ i_c \end{pmatrix} dt \qquad (2)$$

In (2), $\Delta v_a, \Delta v_b$ and $\Delta v_c$ are the series voltage drops along the phases between buses R and S, $i_a, i_b$ and $i_c$ are the phase currents, and $R, L$ and $S$are respectively the phase resistance, inductance and elastance matrix of the circuit. By applying (1) to currents and voltages and rearranging, the following system of equations is obtained:

$$\begin{pmatrix} \Delta v_0 \\ \Delta v_\alpha \\ \Delta v_\beta \end{pmatrix} = \begin{pmatrix} R_0 & 0 & 0 \\ 0 & R_\alpha & 0 \\ 0 & 0 & R_\beta \end{pmatrix} \cdot \begin{pmatrix} i_0 \\ i_\alpha \\ i_\beta \end{pmatrix} + \begin{pmatrix} L_0 & 0 & 0 \\ 0 & L_\alpha & 0 \\ 0 & 0 & L_\beta \end{pmatrix} \cdot \begin{pmatrix} \frac{di_0}{dt} \\ \frac{di_\alpha}{dt} \\ \frac{di_\beta}{dt} \end{pmatrix} + \begin{pmatrix} S_0 & 0 & 0 \\ 0 & S_\alpha & 0 \\ 0 & 0 & S_\beta \end{pmatrix} \cdot \int_{-\infty}^{t} \begin{pmatrix} i_0 \\ i_\alpha \\ i_\beta \end{pmatrix} dt \qquad (3)$$

Eq. (3) can be associated to three uncoupled single-phase circuits, one for each of the new (0, α, β) variables, in place of the original three-phase circuit, as shown in Fig. 1. It could be easily demonstrated that $L_\alpha = L_\beta = L_p - L_m$ and $L_0 = L_p + 2L_m$, with analogous relations holding for resistances and capacitances. Thus, for static symmetrical circuits, parameters R, L, and C in 0, α and β

coordinates coincide with the zero and positive-sequence parameters, respectively. These quantities are usually frequency-dependent: nevertheless, in this paper they are assumed constant even during transient conditions.

Equations (2) and (3), which describe a circuit connected between two buses (a “series” circuit), can be as well referred to a three-phase circuit connected to only one bus of the network (i.e., a “shunt” circuit): $\Delta v_a, \Delta v_b$ and $\Delta v_c$ then become the phase-to-ground voltages at that bus.

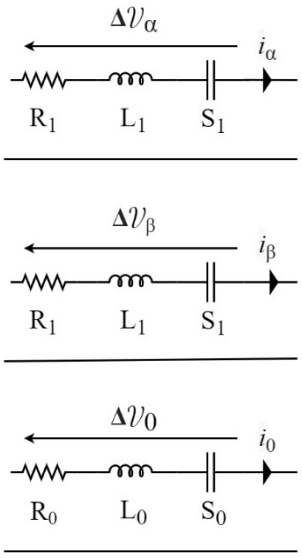


*Fig. 1 Uncoupled 0, α, β equivalent circuit for a symmetrical, three-phase “series” network element.*

In power system studies in which the dynamics of synchronous machines can be neglected, the “rest of the system” is represented through an equivalent emf behind its Thevenin impedance. The application of (1) to three balanced, positive-sequence sinusoidal sources $\overline{E}_a$, $\overline{E}_b$, and $\overline{E}_c$, yields the Clarke equivalent e.m.f.s:

$$\overline{E}_\alpha = \frac{\sqrt{6}}{2}\overline{E}_a$$

$$\overline{E}_\beta = -j \cdot \overline{E}_\alpha \qquad (4)$$

The detailed representation of synchronous machines in Clarke coordinates is more involved and is not treated here.

By consistently applying the transformations just defined to all network elements, three equivalent, single-phase networks, i.e., the 0, α and β component networks are arrived at.

## 3 Single-phase-to-ground fault representation

In terms of symmetrical components, a faulted network is represented by appropriately connecting the sequence networks at fault location, the type of connections depending on the nature of the fault. A similar argument can be made when Clarke 0, α and β component networks are considered instead. A 1LG fault on phase B, for example, is described by the following constraints:

$$v_b = Z_f i_b ; i_a = i_c = 0 \qquad (5)$$

being $Z_f$ the fault impedance, $v_a, v_b, v_c$ the phase voltages to ground at fault location and $i_a, i_b, i_c$ the currents into the fault. In terms of Clarke components, (5) can be rewritten as:

$$v_\alpha = \sqrt{3}\, v_\beta + \sqrt{2}\, v_0 + 6 Z_f i_\alpha ; i_\alpha = \frac{-i_\beta}{\sqrt{3}} = \frac{-i_0}{\sqrt{2}} \qquad (6)$$

Equations (6), referred to 0, α and β quantities at the fault location, are satisfied for the 0, α and β-networks connection shown in Fig. 2, which will be referred to from now on as “Clarke equivalent circuit”.

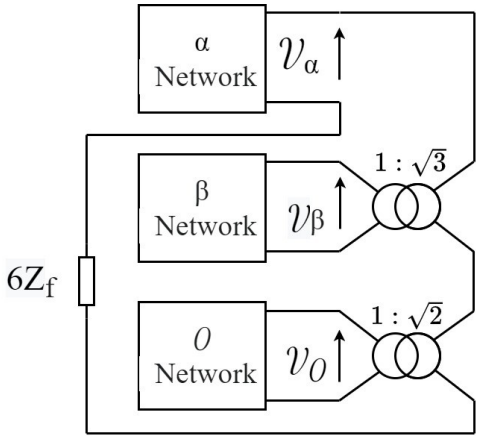


*Fig. 2 Connection of 0, α and β component networks for a 1LG fault on phase B.*

The equivalent networks connection for 1LG faults affecting other phases and, in general, for all other types of faults can be defined by analogous procedures.

## 4 Case study 1

The first case study concerns a 20 kV radial distribution network (“Network 1”), operated with ungrounded neutral and consisting of 5 feeders of different typology (which is quite common in suburban areas in Italy): two overhead lines, an underground cable line and two mixed cable-overhead lines, as shown in Fig. 3. The case was selected with the aim of checking the limits of the proposed lumped-circuit modelling approach, since the network is characterized by some very long MV overhead lines, which would suggest the use of distributed-parameters line representation in the switching transients study [38][39].The line constants of each feeder are reported in Table 1 and nameplate data of the HV/MV transformer are reported in Table 2.

A bolted fault to ground is simulated on phase B at the receiving end of the 50 km-long “A1 - A2” feeder. The resulting overvoltages, both at fault location (bus A2) and at the primary substation (PS) busbars, are investigated by means of the simplified, lumped-parameters Clarke equivalent circuit shown in Figure 4. The α and β networks only include the series impedances of the HV/MV transformer and the faulted feeder (they both coincide with their respective positive-sequence impedances). In this first (introductory) case study, all capacitances in the α and β networks have been disregarded, with the aim to preserve the simplicity of the equivalent circuit. Later, the effects of the α and β-component capacitances on the Clarke equivalent circuit accuracy (and the added computational

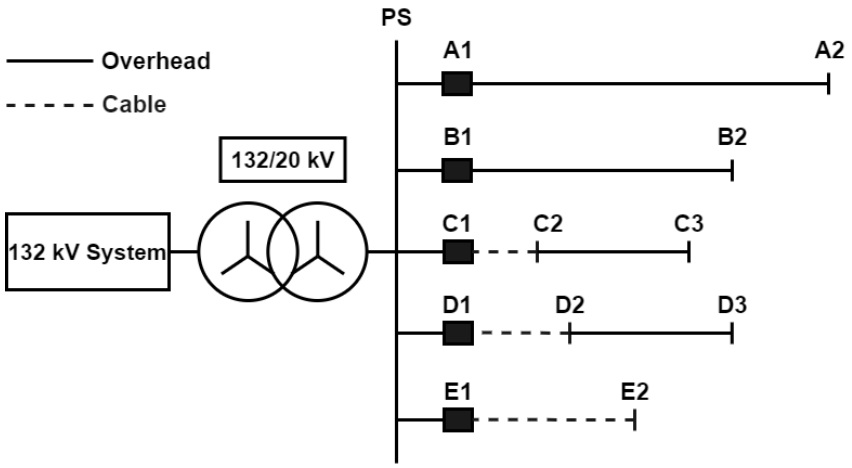


*Fig. 3 Single line diagram of Network 1 (Case study 1).*

*Table 1 Branch lengths and sequence parameters for the Case study 1 network.*

| Section | Length [km] | $R'_0$ [Ω/km] | $X'_0$ [Ω/km] | $C'_0$ [nF/km] | $R'_d$ [Ω/km] | $X'_d$ [Ω/km] | $C'_d$ [nF/km] |
|---|---|---|---|---|---|---|---|
| A1 – A2 | 50 | 0.416 | 1.65 | 4.5 | 0.27 | 0.376 | 9.6 |
| B1 - B2 | 30 | 0.416 | 1.65 | 4.5 | 0.27 | 0.376 | 9.6 |
| C1 – C2 | 5 | 0.828 | 0.22 | 340 | 0.205 | 0.122 | 340 |
| C2 – C3 | 20 | 0.416 | 1.65 | 4.5 | 0.27 | 0.376 | 9.6 |
| D1 – D2 | 10 | 0.828 | 0.22 | 340 | 0.205 | 0.122 | 340 |
| D2 – D3 | 20 | 0.416 | 1.65 | 4.5 | 0.27 | 0.376 | 9.6 |
| E1 – E2 | 20 | 0.828 | 0.22 | 340 | 0.205 | 0.122 | 340 |

*Table 2 HV/MV transformer data*

| | |
|---|---|
| $V_{n1}/V_{n2}$ [kV/ kV] | 132/20 |
| Rated power [MVA] | 40 |
| Short-circuit voltage [%] | 12 |
| Winding connection | Yy |

burden) will be assessed. On the contrary, the 0-component network is represented by the aggregate 0-sequence capacitance of the network and the series 0-sequence impedance of the faulted feeder A1-A2. Network 1 can be considered fed by three balanced voltage sources, to which correspond the α and β equivalent emfs defined by (4). Fault inception is simulated by closing the switch Sw1.

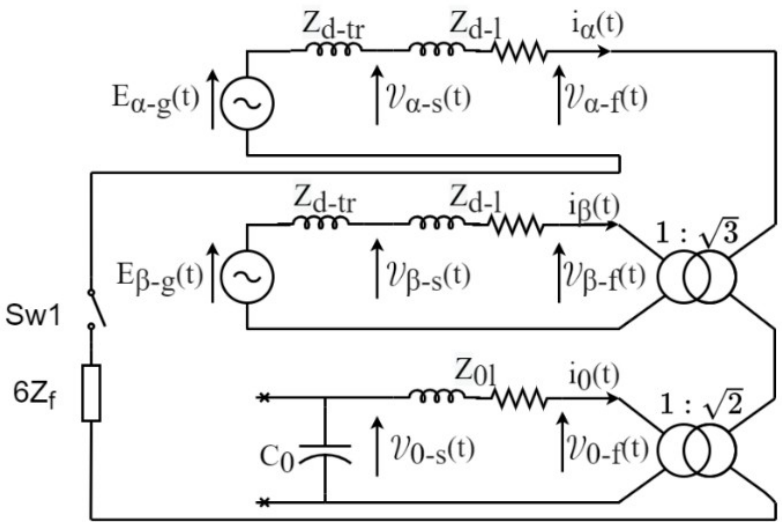


*Figure 4 Equivalent circuit for 1LG fault at bus A2 (phase B). Subscripts "s" and "f" stand for "substation" and "fault point," respectively.*

A complete three-phase model of the Fig. 3 network is necessary as a benchmark to assess the accuracy of the Clarke equivalent circuit simulation results. The question arises whether a constant-parameters distributed line (CPDL, "Bergeron") model can be considered adequate enough or it is necessary to rely on a frequency-dependent model (ULM, Universal Line Model). Thus, the 1LG fault at bus A2 – phase B of the Fig. 3 network has been simulated both by means of ATP (CP models) and EMTP-RV (ULM): healthy phase voltage waveforms simulated at fault location are reported in Fig. 5. The comparison evidences that discrepancies between the two models are very limited when short circuits in the MV lines are simulated, the CP model is hence taken as a benchmark in this paper due to its satisfactory accuracy and lower computation times (for the simulations in Fig. 5, computation time is 128 seconds for CDPL and 1146 seconds for ULM).

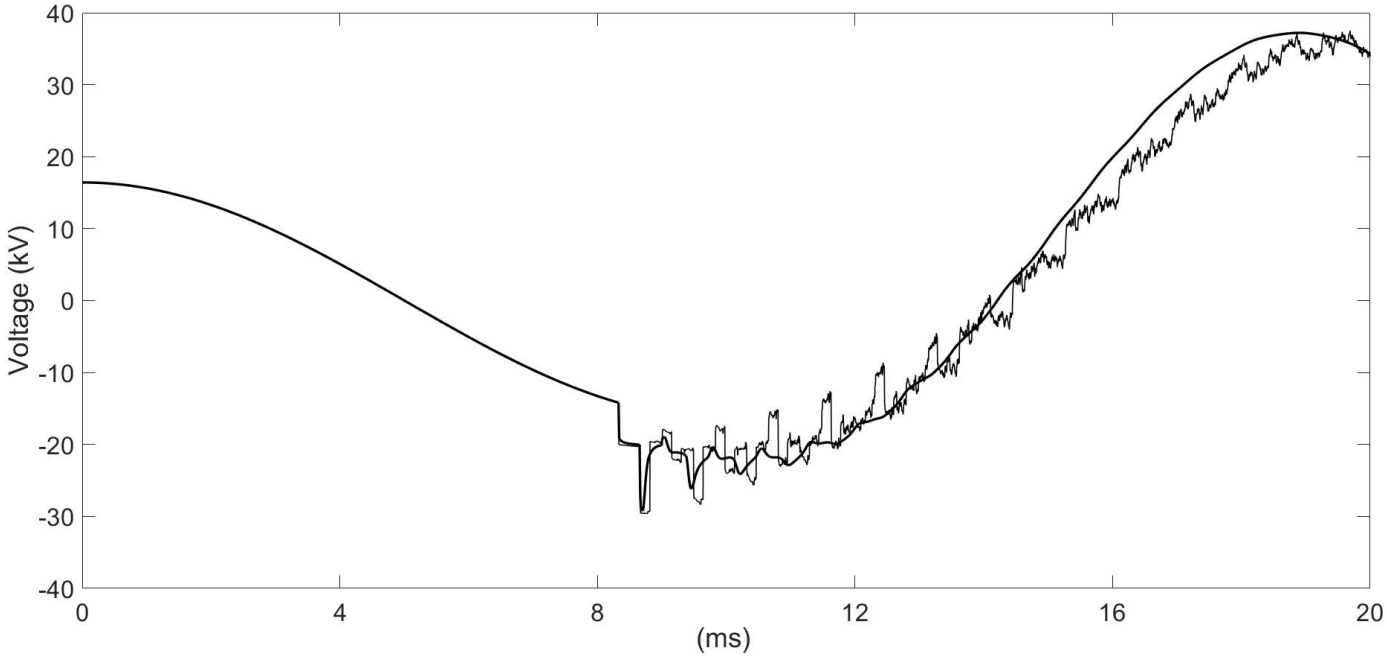


*Figure 5 Case study 1. Waveforms of phase A voltage to ground at fault location, following a bolted phase-B 1LG fault at bus A2. Comparison between CP model (thin line) and ULM (thick line).*

The 1LG fault scenario has thus been simulated by means of a complete three-phase circuit model of Network 1. Individual line stretches have been implemented as (type -1, -2, -3) distributed-parameters elements and the HV/MV transformer simulated as a “saturable transformer” component [18]. Both the benchmark model and the Clarke equivalent circuits have been solved with 0.1 μs time-step and 0.2 s total simulation time.

Voltage waveforms yielded by the two circuits are compared in Fig. 6, which reports the time plot of phase-A voltage at fault location, and Fig. 7, reporting the plot of phase-A voltage at PS busbars.

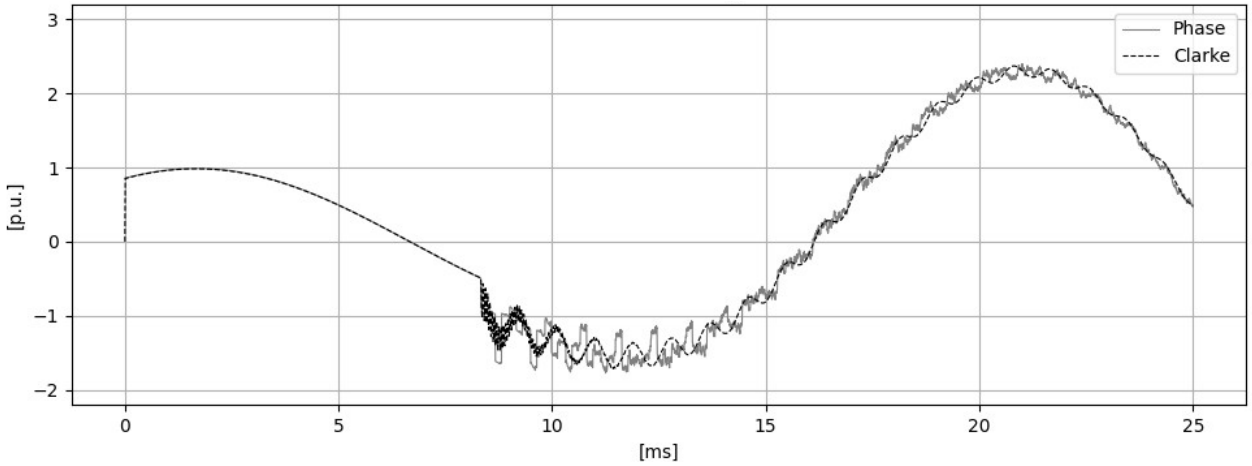


*Fig. 6 Case study 1. Phase A voltage to ground at fault location, following a bolted phase-B 1LG fault at bus A2.*

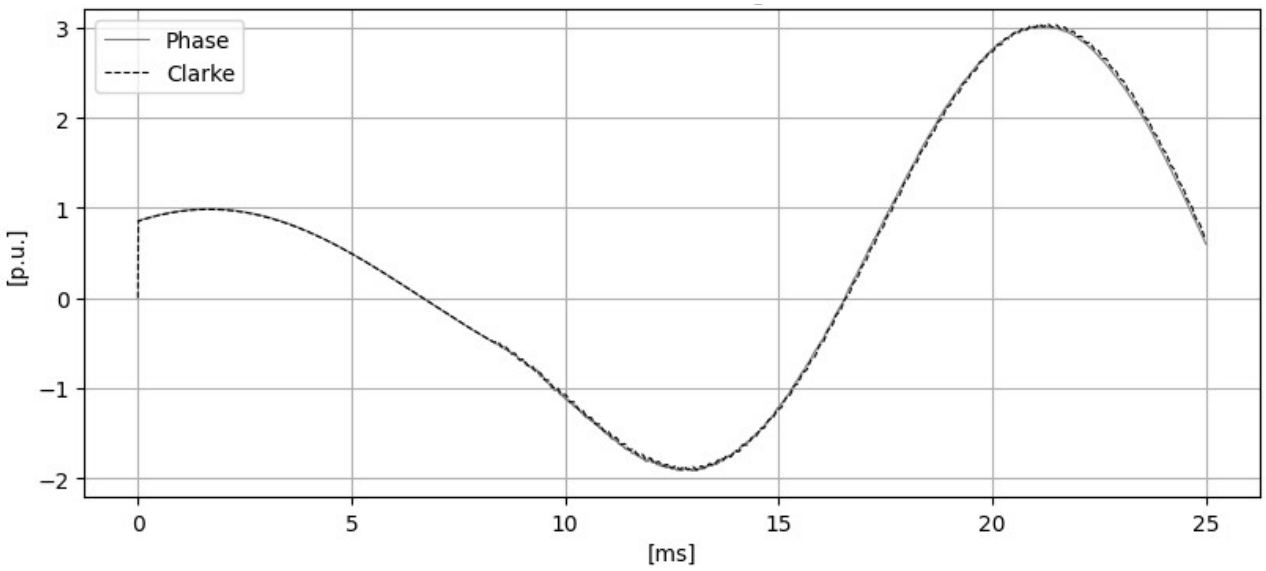


*Fig. 7 Case study 1. Phase A voltage to ground at PS busbars, a bolted phase-B 1LG fault at bus A2.*

As expected, the Clarke equivalent circuit allows to reproduce satisfactorily the “low-frequency” components of the transient, i.e., the smooth transition from the pre-fault steady-state voltage to the faulty steady-state temporary overvoltage. On the other hand, high-frequency components are reproduced in a markedly different manner, as evidenced by the detail reported in Fig. 8:

- in the complete three-phase simulation, the high-frequency square-wave patterns associated with multiple reflections and refractions of travelling waves along the faulty line are clearly visible:

- voltage waveforms yielded by the Clarke equivalent circuit only exhibit high-frequency damped oscillations associated with the natural frequencies of the RLC series circuit of Figure 4.

Comparing the waveforms of Fig. 6 and Fig. 7, it is apparent that high-frequency voltage components are far less noticeable at the busbars because the capacitance to ground of the sound feeders offers a low-impedance path to high-frequency current waves. Since in a radial MV network operated with ungrounded neutral the maximum transient overvoltages due to 1LG faults occur at the PS busbars, where Clarke equivalent circuits proved to be very accurate, the application of the proposed method can be considered adequate enough for fault studies concerning such networks.

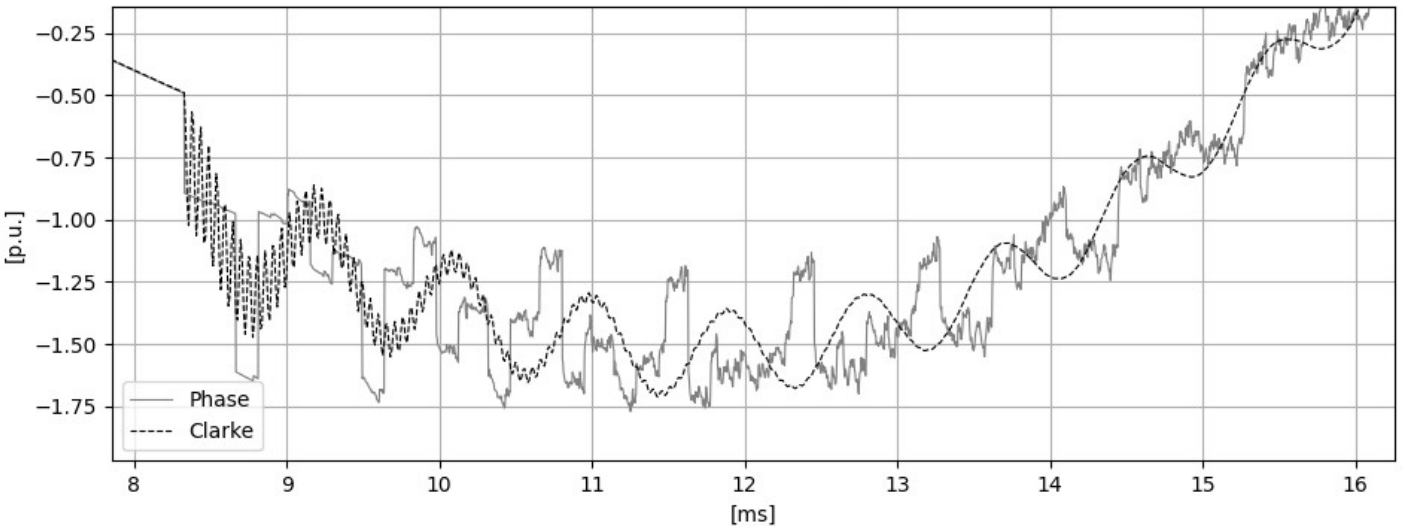


*Fig. 8 Case study 1. Detail of phase A voltage to ground at fault location, following a bolted phase-B 1LG fault at bus A2.*

## 5 Case study 2

The second case study deals with the parametric evaluation of transient overvoltages caused by 1LG faults in another existing Italian MV distribution network (“Network 2”), also operated with ungrounded neutral, by means of the simplified Clarke equivalent circuit described in the previous section.

The DSO repeatedly pointed out the occurrence of dangerous overvoltages, with several instances of temporary or switching overvoltages due to ground faults causing subsequent faults on the healthy

phases, at other locations in the network. These occurrences were confirmed by simulations and fully replicated by staging faults [36].

Network 2 is located in a suburban area and consists mostly of underground cable lines, plus a few long overhead lines. The total zero-sequence capacitance of the network is 35650 nF and the attendant capacitive 1LG fault current, neglecting all longitudinal impedances, is 388 A at 20 kV. HV/MV transformer nameplate data are reported in Table 2. Lengths and electrical constants of the different sections are reported in Table 3. Network 2 is characterized by electrically short line segments, liable to multiple reflections of the travelling waves which will not be considered in the Clarke simplified representation. With the exception of the faulted line, the network model inputted into the Clarke transformations consists of the simple sequence-based equivalents used for unsymmetrical fault calculations.

1LG faults have been simulated at bus V 54, i.e., at the receiving end of the 16 km-long feeder depicted in Fig. 9, which is almost completely in overhead execution.

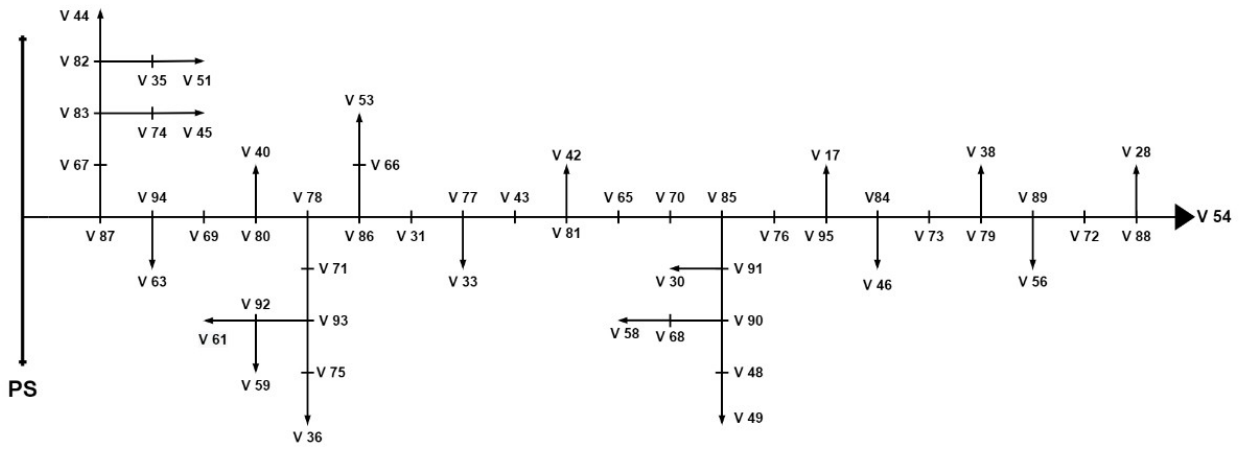


*Fig. 9 Case study 2. Single line diagram of the faulted MV feeder*

*Table 3 Case study 2. Branch lengths and sequence parameters for the different segments of the faulted line in Fig. 9.*

| Section | Length [km] | $R'_0$ [Ω/km] | $X'_0$ [Ω/km] | $C'_0$ [nF/km] | $R'_d$ [Ω/km] | $X'_d$ [Ω/km] | $C'_d$ [nF/km] |
|---|---|---|---|---|---|---|---|
| PS – V 87 | 2.657 | 0.56 | 1.38 | 74.5 | 0.21 | 0.33 | 79.2 |

| | | | | | | | |
|---|---|---|---|---|---|---|---|
| V 87 – V 94 | 0.27 | 0.67 | 1.61 | 4.1 | 0.52 | 0.39 | 9.1 |
| V 94 – V 69 | 0.04 | 0.60 | 1.60 | 4 | 0.60 | 0.40 | 8 |
| V 69 – V 80 | 0.38 | 0.66 | 1.62 | 4 | 0.52 | 0.39 | 9 |
| V 80 – V 78 | 0.57 | 0.67 | 1.61 | 4.1 | 0.51 | 0.38 | 8.9 |
| V 78 – V 86 | 0.25 | 0.67 | 1.62 | 4.1 | 0.51 | 0.38 | 8.9 |
| V 86 – V 31 | 4.18 | 0.67 | 1.62 | 4 | 0.52 | 0.39 | 9 |
| V 31 – V 77 | 1.12 | 0.69 | 1.61 | 4.9 | 0.52 | 0.38 | 12.3 |
| V 77 – V 43 | 0.45 | 0.67 | 1.62 | 4.1 | 0.52 | 0.38 | 9 |
| V 43 – V 81 | 0.5 | 0.66 | 1.62 | 4 | 0.52 | 0.40 | 9.1 |
| V 81 – V 65 | 0.1 | 0.67 | 1.64 | 3.2 | 0.72 | 0.41 | 8 |
| V 65 – V 70 | 1.4 | 0.88 | 1.63 | 3 | 0.72 | 0.41 | 8 |
| V 70 – V 85 | 0.55 | 0.87 | 1.65 | 3 | 1.05 | 0.41 | 8 |
| V 85 – V 76 | 0.31 | 1.19 | 1.65 | 3.1 | 1.12 | 0.42 | 8 |
| V 95 – V 84 | 0.65 | 1.26 | 1.65 | 3.1 | 1.12 | 0.43 | 8 |
| V 73 – V 79 | 0.15 | 1.27 | 1.65 | 3.2 | 1.12 | 0.42 | 8 |
| V 79 – V 89 | 0.9 | 1.25 | 1.65 | 3 | 1.12 | 0.42 | 8 |
| V 89 – V 72 | 0.65 | 1.27 | 1.65 | 3 | 1.12 | 0.41 | 8 |
| V 88 – V 54 | 0.88 | 0.87 | 1.63 | 3 | 0.72 | 0.40 | 8 |

The 1LG fault simulations at bus V54 have been repeated for different fault inception times and fault resistance value:

- fault inception instants have been varied at 30 electrical degrees intervals, starting with the pre-fault phase voltage being at its peak.
- 10 logarithmically spaced fault resistances between 1Ω and 100Ω have been simulated.

For Case study 2 a more detailed lumped-parameters Clarke equivalent circuit (compared to the circuit in Figure 4) has been set up, which also includes the shunt capacitances in the α and β-networks as shown in Fig. 10. The Clarke equivalent network has been hand-synthesized for this case but an automatic procedure, which take into account the available network data format and the specific EMT software, would be easily implementable.

To evaluate the effects of the shunt capacitances on the overall accuracy of the equivalent circuit, results yielded by the circuit of Fig. 10 (“Clarke-pi” equivalent circuit) are compared with those obtained from the equivalent circuit already used in the first case study (“Clarke-series” equivalent

circuit, represented in Figure 4). Moreover, all simulations were also repeated on a complete three-phase, distributed-parameter circuit model of Network 2, acting as a benchmark. In all cases total simulation time was 0.2 s with 0.1 μs time-step.

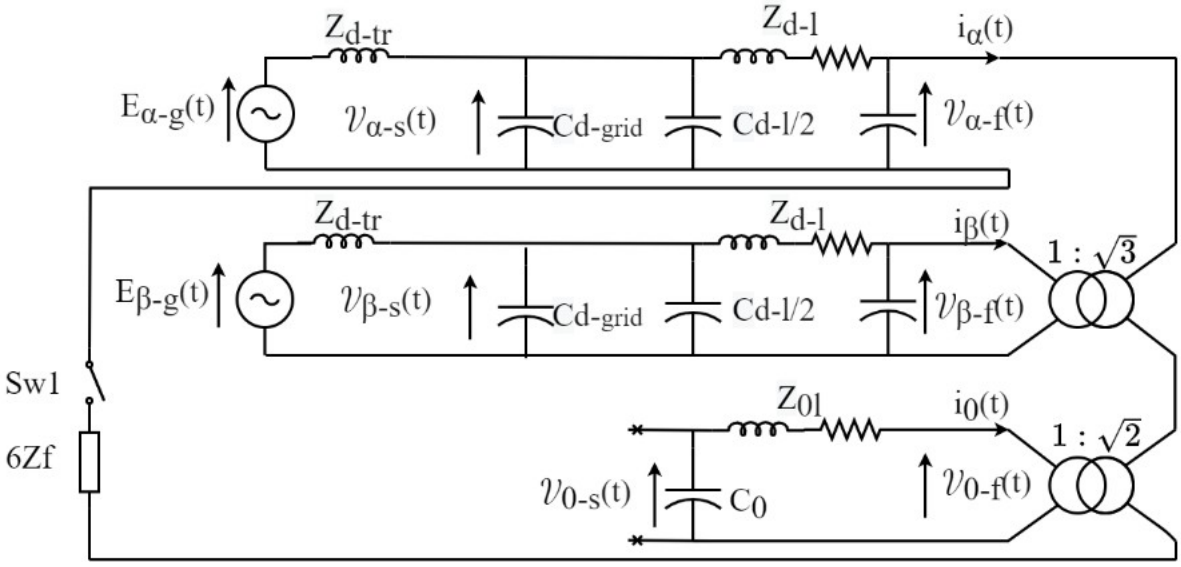


*Fig. 10 Case study 2. "Clarke-pi" equivalent circuit for a phase-B 1LG fault at BUS V54. Subscripts "s" and "f" stand for substation and fault point, respectively*

Fig. 11 and Fig. 12 report the voltage waveforms associated to the worst-case 1LG fault (inception at peak faulted phase voltage, 1 Ω fault resistance).

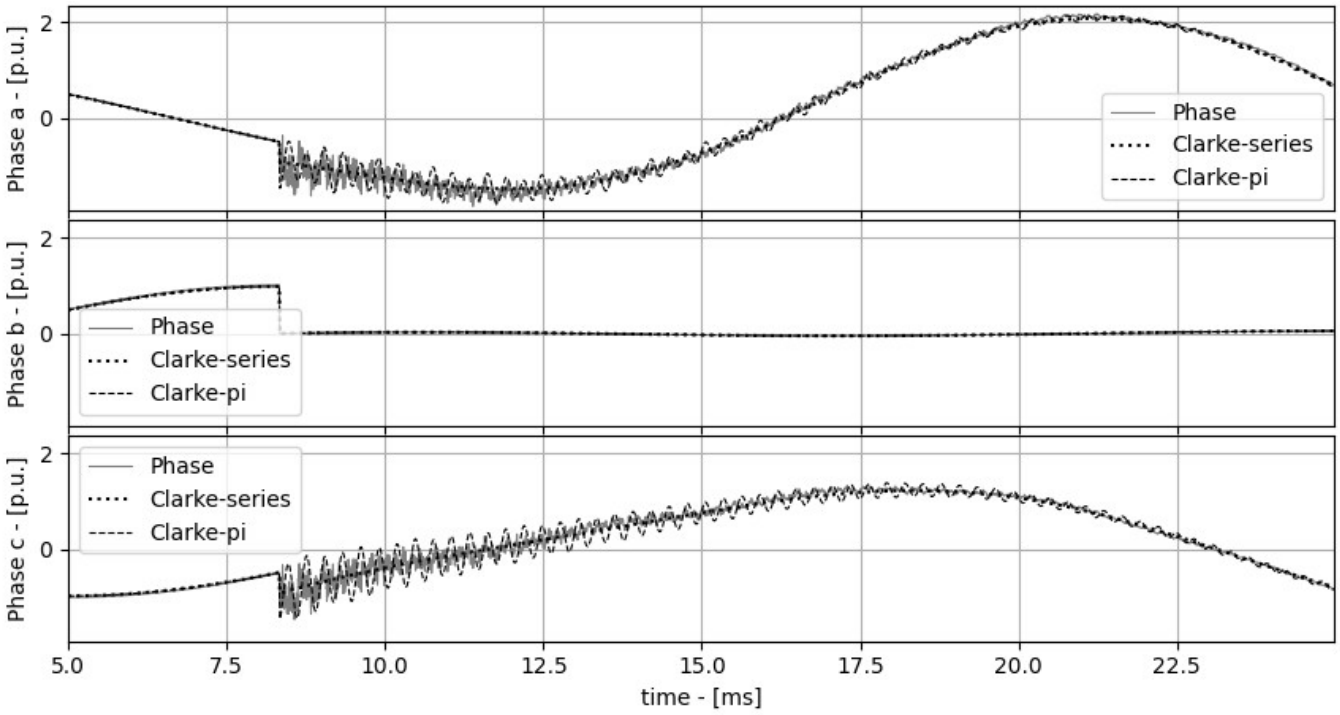


*Fig. 11 Case study 2. Voltages to ground computed at fault location for a 1LG fault at bus V54. Comparison between three-phase complete circuit, Clarke-series equivalent circuit, Clarke-pi equivalent circuit (see text for details).*

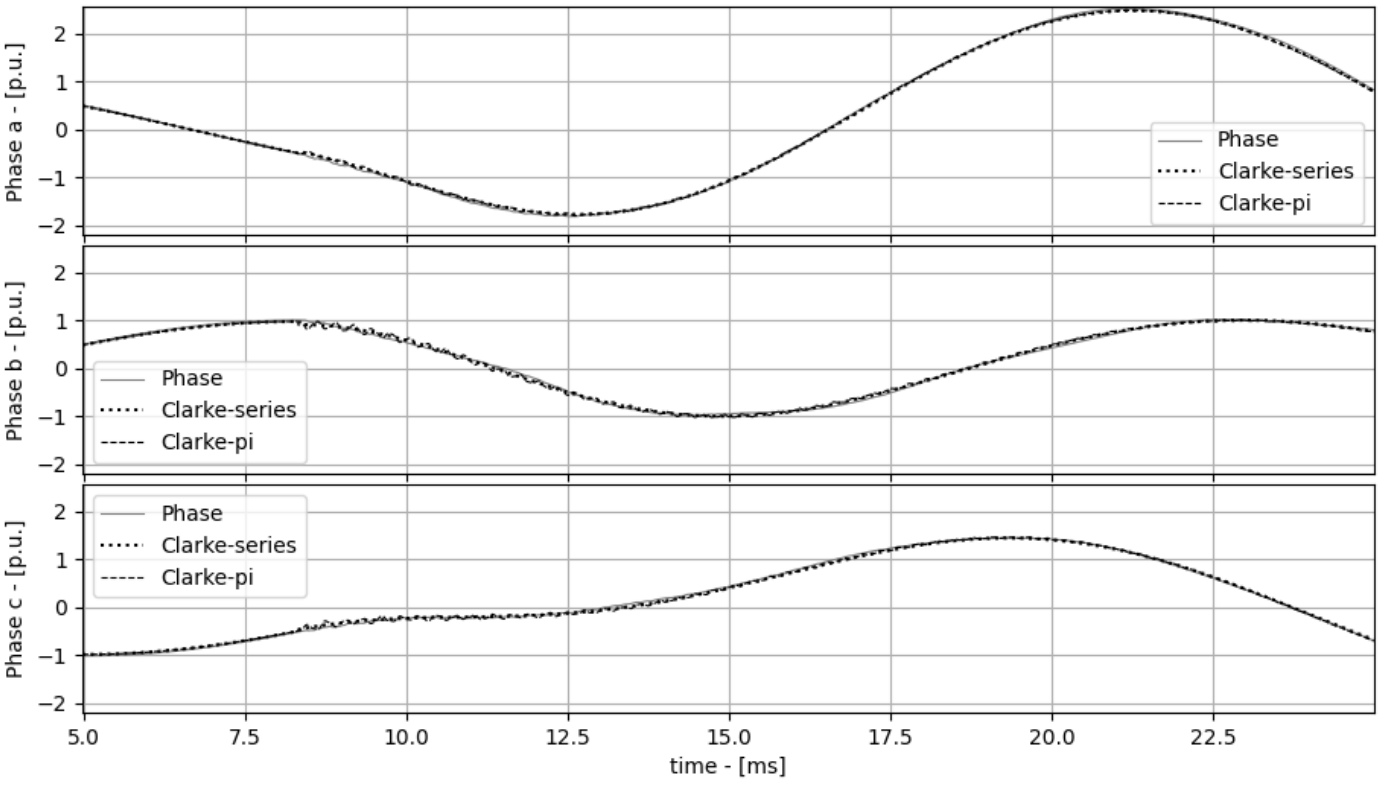


*Fig. 12 Case study 2. Voltages to ground computed at PS busbars for a 1LG fault at bus V54. Comparison between three-phase complete circuit, Clarke-series equivalent circuit, Clarke-pi equivalent circuit.*

As in the previous case, voltages yielded by the Clarke equivalent circuits correctly follow the aperiodic, low-frequency transient, both at fault location and at PS busbars.

The comparison between transient simulation results for an end-of-line fault in Fig. 11 shows that the "Clarke-series" circuit (where the faulted feeder capacitances have been neglected) does not reproduce satisfactorily the healthy phase voltages at fault location. The busbar voltage waveforms yielded by the "Clarke-series" circuit are, however, acceptable as shown in Fig. 13. The model can thus be used to evaluate peak overvoltages at the MV busbars. As in the previous case the purpose is using the simplest possible model instead than going for the full network representation (as in the benchmark) or opting for a frequency-dependent network equivalent [40-43]

Although the Clarke-pi equivalent circuit computes well the amplitude of the high-frequency harmonics, it does not reproduce the correct waveform, as shown in the detail reported in Fig. 12. As mentioned before, this is due to the concentrated nature of the line model in the 0, α and β components. This behaviour is far less noticeable at the PS busbars, where the maximum overvoltage value is found, again as in case study 1.

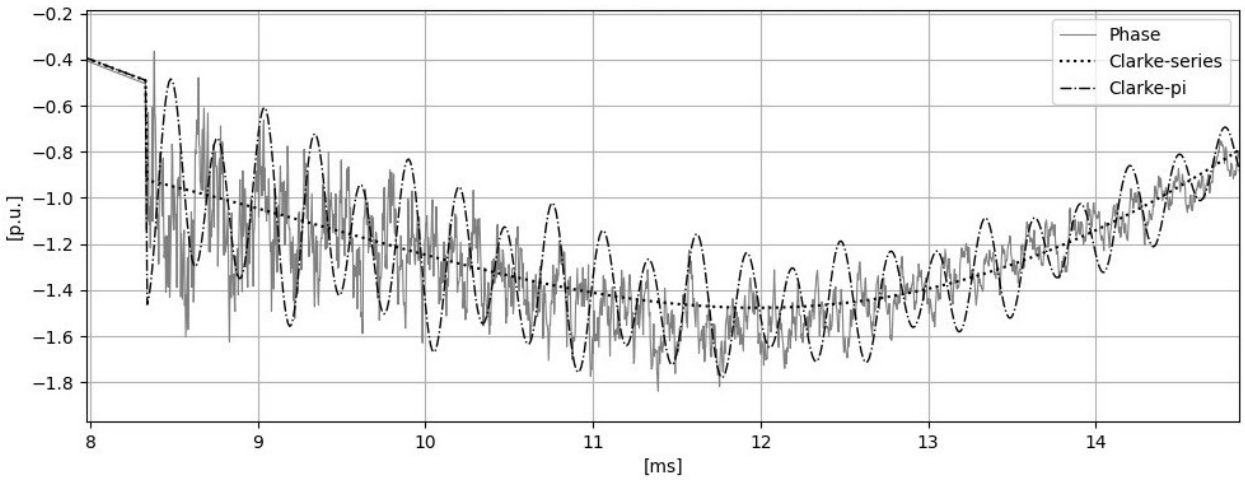


*Fig. 13 Case study 2. Detail of phase A voltage to ground reported in Fig. 11.*

For this Case study 2 another fault scenario has been taken into account. Fig. 14 shows the Clarke equivalent circuit for a 1LG fault on phase B at the PS busbars, and Fig. 15 compares the attendant

voltage waveforms yielded by the Clarke-pi equivalent circuit and the complete three-phase model. It is apparent that the accuracy of the lumped-parameter equivalent circuit is slightly worse in this second scenario. This is ascribable to the fact that the Clarke equivalent circuit is not well damped, having neglected all the feeders series impedances, with their non-negligible series resistances.

It can be stated that the farther the 1LG fault is from the PS busbars, the smaller the mismatch between overvoltages at PS busbars yielded by the Clarke equivalent circuit and, respectively, the complete three phase model of the network. In most cases, accuracy is very good, especially if compared to the accuracy of overvoltages calculated at fault location.

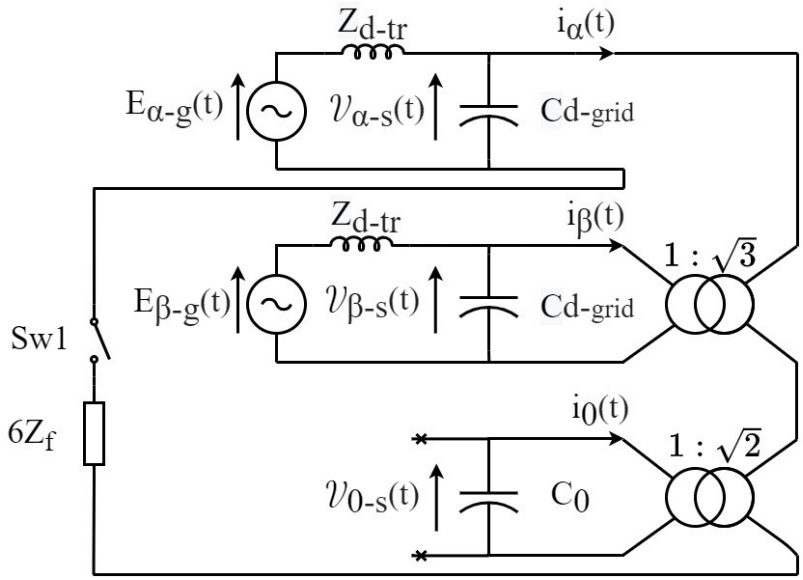


*Fig. 14 Case study 2. Clarke equivalent circuit for the simulated phase-B 1LG fault at the PS busbars (see text for details).*

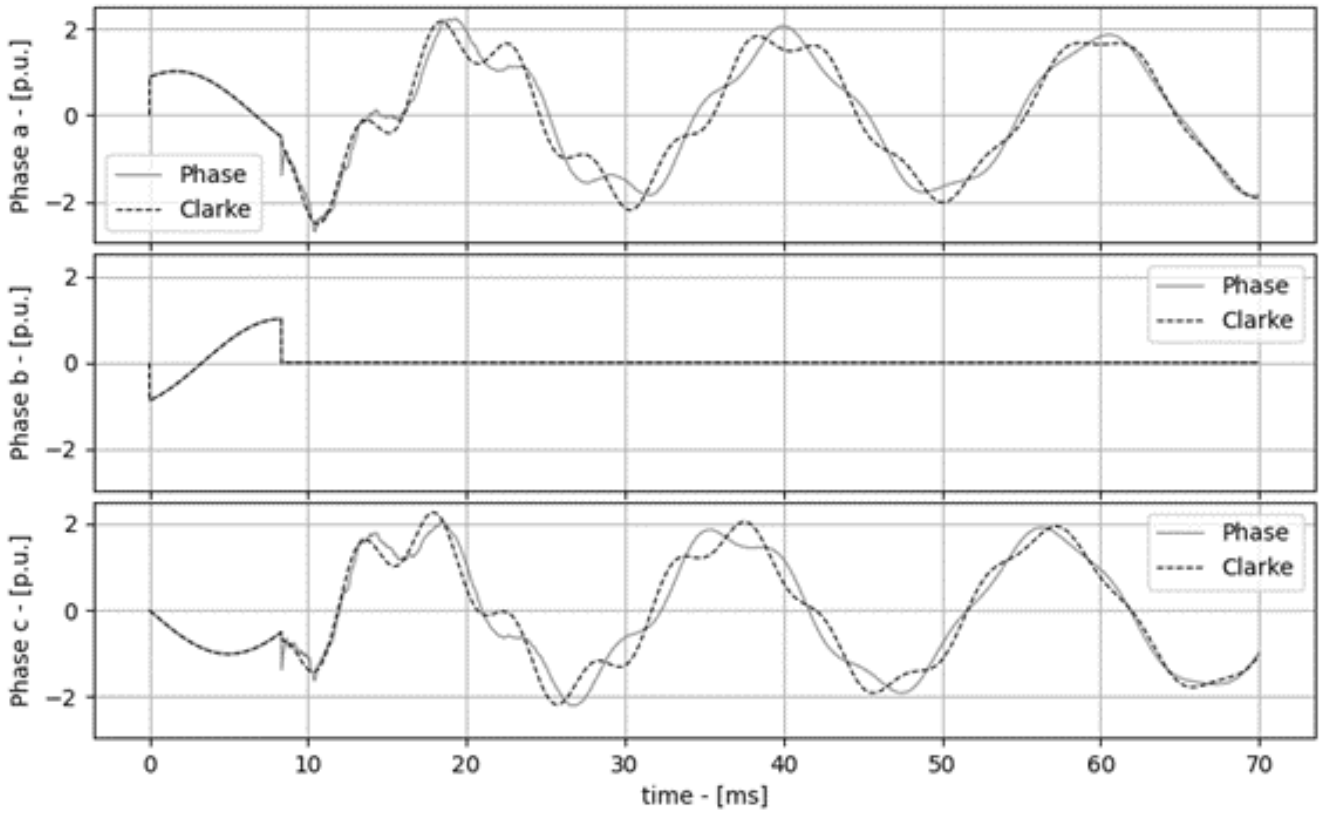


*Fig. 15 Case study 2. Phase voltages following a phase-B 1LG fault at the PS busbars.*

Table 4 and Table 5 report the mismatch between peak healthy phase overvoltages at fault location, yielded by the Clarke-pi equivalent and the three-phase distributed-parameter circuit for the 1LG fault at bus V54 on phase B. A similar comparison is reported in Table 6 for phase A overvoltages computed at the PS busbars. All mismatches are calculated as:

$$\Delta V_{\%} = \frac{\left(Vpk_{three-phase} - Vpk_{clarke-pi}\right)}{\left(Vpk_{three-phase}\right)} \cdot 100 \qquad (7)$$

*Table 4 Case study 2. Percent difference between benchmark and Clarke-pi peak phase-A voltages at fault location (1LG fault at Bus V54).*

| | *Fault inception phase (degree)* | | | | | | | | | | | |
|---|---|---|---|---|---|---|---|---|---|---|---|---|
| $Z_f$ (Ω) | 0 | 30 | 60 | 90 | 120 | 150 | 180 | 210 | 240 | 270 | 300 | 330 |
| *1* | -0.83 | -2.34 | -1.19 | -1.89 | -2.09 | -0.09 | -0,84 | -2.33 | -1.20 | -1.89 | -2.10 | -0.08 |
| *2.5* | -1.05 | -2.60 | -1.46 | -1.87 | -2.28 | -0.45 | -1,05 | -2.59 | -1.46 | -1.87 | -2.29 | -0.43 |
| *4* | -1.27 | -2.83 | -1.57 | -1.87 | -2.27 | -0.77 | -1,26 | -2.81 | -1.57 | -1.87 | -2.28 | -0.76 |
| *6,3* | -1.59 | -2.08 | -1.78 | -1.86 | -2.23 | -1.39 | -1,57 | -2.07 | -1.78 | -1.86 | -2.23 | -1.40 |
| *10* | -1.55 | -1.86 | -2.16 | -1.87 | -2.21 | -2.24 | -1,53 | -1.85 | -2.16 | -1.87 | -2.21 | -2.23 |
| *16* | -1.55 | -2.50 | -2.31 | -1.94 | -2.18 | -2.72 | -1,56 | -2.50 | -2.30 | -1.94 | -2.18 | -2.71 |
| *25* | -1.56 | -3.30 | -1.99 | -2.49 | -2.15 | -3.17 | -1,57 | -3.28 | -1.99 | -2.49 | -2.14 | -3.17 |
| *40* | -1.48 | -3.58 | -2.46 | -2.47 | -2.79 | -0.30 | -1,47 | -3.53 | -2.45 | -2.47 | -2.79 | -0.31 |

| | | | | | | | | | | | | |
|---|---|---|---|---|---|---|---|---|---|---|---|---|
| *63* | -1.89 | -5.01 | -2.72 | -2.58 | -3.12 | -1.14 | -1,89 | -4.46 | -2.72 | -2.58 | -3.12 | -1.16 |
| *100* | -3.30 | -4.17 | -2.89 | -2.69 | -3.07 | -1.96 | -3,32 | -3.80 | -2.89 | -2.69 | -3.08 | -1.93 |

*Table 5 Case study 2. Percent difference between benchmark and Clarke-pi peak phase-C voltages at fault location (1LG fault at Bus V54).*

| | *Fault inception phase (degree)* | | | | | | | | | | | |
|---|---|---|---|---|---|---|---|---|---|---|---|---|
| $Z_f$ (Ω) | 0 | 30 | 60 | 90 | 120 | 150 | 180 | 210 | 240 | 270 | 300 | 330 |
| *1* | 0.67 | 0.02 | -0.32 | -1.04 | -4.74 | 2.65 | 0.67 | 0.02 | -0.33 | -1.04 | -4.05 | 3.87 |
| *2.5* | 0.32 | -0.35 | -0.49 | -1.20 | -4.57 | 3.07 | 0.31 | -0.34 | -0.49 | -1.20 | -3.81 | 4.29 |
| *4* | -0.02 | -0.91 | 1.24 | -2.80 | -4.41 | 3.47 | -0.03 | -0.89 | 1.39 | -2.80 | -3.59 | 4.69 |
| *6,3* | -3.26 | -1.24 | 1.13 | -3.04 | -4.18 | 4.03 | 2.72 | -1.22 | 1.24 | -3.04 | -3.26 | 5.26 |
| *10* | -2.77 | 4.75 | 1.20 | -2.89 | -3.83 | 4.84 | 8.14 | 4.69 | 1.33 | -2.89 | -2.78 | 6.08 |
| *16* | -2.02 | 2.18 | 1.26 | -2.84 | -3.33 | 5.92 | 10.15 | 2.26 | 1.40 | -2.84 | -2.12 | 7.20 |
| *25* | -0.98 | -0.52 | 0.82 | -2.73 | -2.66 | 7.11 | 12.51 | -0.43 | 0.66 | -2.73 | -1.29 | 8.44 |
| *40* | 0.57 | -2.65 | -0.65 | -2.74 | -1.85 | 8.28 | 12.82 | -2.61 | -0.73 | -2.74 | -0.39 | 9.66 |
| *63* | 2.52 | -4.20 | -2.85 | -2.62 | -1.07 | 8.82 | 5.31 | -4.19 | -2.90 | -2.62 | 0.33 | 10.04 |
| *100* | -5.76 | -5.56 | -4.70 | -2.76 | -0.48 | 8.04 | -5.77 | -5.57 | -4.73 | -2.76 | 0.66 | 9.14 |

*Table 6 Case study 2. Percent difference between benchmark and Clarke-pi peak phase-A voltages at the PS busbars (1LG fault at Bus V54).*

| | *Fault inception phase (degree)* | | | | | | | | | | | |
|---|---|---|---|---|---|---|---|---|---|---|---|---|
| $Z_f$ (Ω) | 0 | 30 | 60 | 90 | 120 | 150 | 180 | 210 | 240 | 270 | 300 | 330 |
| *1* | -0.50 | -2.11 | 1.68 | -1.82 | -1.40 | 2.12 | -0.49 | -2.11 | 1.68 | -1.82 | -1.40 | 2.12 |
| *2.5* | -1.52 | -2.70 | 1.06 | -1.73 | -1.78 | 1.09 | -1.52 | -2.70 | 1.06 | -1.73 | -1.78 | 1.09 |
| *4* | -2.84 | -3.03 | 0.46 | -1.80 | -2.00 | -0.22 | -2.84 | -3.03 | 0.46 | -1.80 | -2.00 | -0.22 |
| *6,3* | -2.78 | -3.09 | -0.80 | -0.96 | -2.21 | -2.15 | -2.78 | -3.09 | -0.80 | -0.96 | -2.21 | -2.15 |
| *10* | -2.68 | -2.05 | -2.54 | -1.31 | -1.25 | -3.19 | -2.68 | -2.05 | -2.54 | -1.31 | -1.25 | -3.19 |
| *16* | -2.52 | 0.19 | -3.23 | -2.03 | -1.57 | -3.58 | -2.52 | 0.19 | -3.23 | -2.03 | -1.56 | -3.58 |
| *25* | -2.30 | -0.58 | -2.56 | -2.55 | -1.25 | -1.70 | -2.30 | -0.58 | -2.56 | -2.55 | -1.25 | -1.70 |
| *40* | -1.98 | -2.43 | -1.45 | -2.66 | -2.67 | -1.82 | -1.98 | -2.43 | -1.45 | -2.66 | -2.67 | -1.82 |
| *63* | -1.56 | -3.16 | -1.43 | -2.50 | -3.02 | -0.23 | -1.56 | -3.16 | -1.43 | -2.50 | -3.02 | -0.23 |
| *100* | -1.05 | -3.23 | -1.95 | -2.42 | -2.88 | -1.81 | -1.05 | -3.23 | -1.95 | -2.42 | -2.88 | -1.81 |

The above results show that the Clarke model computes effectively the peak overvoltages, with an error always lower than 4% for phase A, i.e., the phase affected by the largest overvoltages. This result is achieved with a much simpler model than the complete three-phase model (22 buses vs. 1020 buses); the size of the Clarke-pi model is comparable to the usual sequence-based equivalent circuit used for steady-state fault calculations and it uses the same data. As a consequence, computation times are drastically reduced, which might be useful in large-scale parametric studies. In particular, on the

laptop with an Intel Core i7-8565U 1.80 GHz CPU and 8 GB RAM used in this study, the average computation time needed to simulate one 1LG fault with the three-phase circuit was 128.7 seconds, while Clarke-series circuit and Clarke-pi-circuit took an average 4.2 s and 4.5 s computation time, respectively. In the parametric study for network 2, if 1LG faults are simulated at each bus for three different fault resistance values (e.g., 5 Ω, 10 Ω and 30 Ω), the complete three-phase circuit would require a total 1020·3·128.7 s computation time, i.e., about 110 hours. By using the Clarke equivalent circuit presented in this paper, the same study would be performed in about 4 hours, with a 96% time saving.

## 6 Conclusions

Simplified single-phase lumped-parameter circuits based on the Clarke transform have been used to study transient overvoltages due to 1LG faults in a 20 kV network operated with ungrounded neutral. A parametric study based on time-domain simulations of the Clarke equivalent circuit, simultaneously varying fault resistance and inception time, has been carried out. Results obtained have been compared to those yielded by a complete three-phase model. The main findings are:

- the simplified Clarke model (faulted line plus aggregate network capacitance) correctly reproduces the main voltage transient which results in large temporary overvoltages on the healthy phases, both at fault location and at PS busbars;
- Although lumped-parameter circuits cannot reproduce propagation phenomena associated with distributed-parameter transmission lines, higher frequency transient components can be satisfactorily approximated if the alpha and beta-component capacitances are included in Clarke circuits. At any rate, for the end-of-line fault, differences are much less marked at the PS busbars, where maximum overvoltages are found;
- for the studied case, use of simplified lumped-parameters Clarke equivalent circuits drastically reduces modelling effort and computation times. The latter point might be of interest for large-scale parametric studies.

## Bibliography


[1] C. L. Fortescue, “Method of symmetrical coordinates applied to the solution of polyphase networks,” Trans. Am. Inst. Electr. Eng., vol. 37, pp. 1027–1140, 1918.

[2] E. Clarke, “Determination of Voltages and Currents During Unbalanced Faults,” Gen. Electr. Rev., pp. 511–513, 1937.

[3] E. Clarke, “Problems Solved by Modified Symmetrical Components,” Gen. Electr. Rev., vol. 53, no. 9, pp. 488–494, 1938.

[4] E. W. Kimbark, “Two-phase co-ordinates of a three-phase circuit,” Electr. Eng., vol. 58, no. 11, pp. 894–910, Nov. 1939.

[5] N. Koga, "Transformation circuit of α, β and 0 component and its applications," Ohm (Tokio, Japan), Vol. 43, 1956, pp.235

[6] N. Rama Rao and P. S. R. Murthy, “Double unbalances and transient analysis of power systems using R,S,T components,” Proc. Inst. Electr. Eng., vol. 114, no. 6, p. 755, 1967.

[7] L. A. Pipes, “Transient Analysis of Symmetrical Networks by the Method of Symmetrical Components,” Trans. Am. Inst. Electr. Eng., vol. 59, no. 8, pp. 457–459, 1940.

[8] W. P. Lewis, "Solution of network transients using symmetrical components techniques," IEE Proc., vol. 113, 1966

[9] C. L. Fortescue, discussion of E. W. Boehne's paper, "The determination of circuit recovery rates," Trans. A.I.E.E., vol. 54, 1935, pp.530; appearing in Vol. 55 (1936), pp. 192

[10] R. D. Evans and A. C. Monteith, “System Recovery Voltage Determination by Analytical and A-C Calculating Board Methods,” Trans. Am. Inst. Electr. Eng., vol. 56, no. 6, pp. 695–705, 1937.

[11] P. Hammarlund, Transient Recovery Voltage, vol. 1. Acta Polytechnica, El. Eng. Series, 1947.

[12] L. A. Pipes, "Transient Analysis of Completely Transposed Multiconductor Transmission Lines," A.I.E.E. Transactions, vol. 60, pp. 346-351, 1941

[13] J. Fallou, “Propagation des Courant de Haute Frequence Polyphases le Long des Lignes Aeriennes de Transport d’Energie Affectees de Court-circuits ou de Defauts d’Isolement,” Societe Francaise des Electriciens, No. 2, pp.787 – 864, 1932.

[14] A. Greenwood, "Electrical Transients in Power Systems," Wiley, 1991

[15] E. T. B. Gross and L. Rabins, “Transient analysis of three-phase power systems, part I,” J. Franklin Inst., vol. 251, no. 3, pp. 333–341, Mar. 1951.

[16] L. Rabins and E. T. B. Gross, “Transient analysis of three-phase power systems, part II,” J. Franklin Inst., vol. 251, no. 5, pp. 521–537, 1951.

[17]E. Clarke, C. N. Weygandt and C. Concordia, "Overvoltages caused by unbalanced short circuits: Effect of amortisseur windings," in Electrical Engineering, vol. 57, no. 8, pp. 453-468, Aug. 1938

[18]W. C. Duesterhoeft, M. W. Schulz and E. Clarke, "Determination of Instantaneous Currents and Voltages by Means of Alpha, Beta, and Zero Components," in Transactions of the American Institute of Electrical Engineers, vol. 70, no. 2, pp. 1248-1255, July 1951

[19] P. Krause, O. Wasynczuk, S. D. Sudhoff, Steven Pekarek, “Analysis of Electric Machinery and Drive Systems,” Wiley-IEEE Press, 2013

[20] V. K. Sood, “Hvdc and Facts Controllers: Applications Of Static Converters In Power Systems,” Springer, 2013

[21] R. Teodorescu, M. Liserre, P. Rodriguez, “Grid Converters for Photovoltaic and Wind Power Systems,” Wiley-IEEE Press, 2007

[22]J. M. Aller, A. Bueno and T. Paga, "Power system analysis using space-vector transformation," in IEEE Transactions on Power Systems, vol. 17, no. 4, pp. 957-965, Nov. 2002

[23] M. H. J. Bollen and I. Y. Gu, "On the Analysis of Voltage and Current Transients in Three-Phase Power Systems," in *IEEE Transactions on Power Delivery*, vol. 22, no. 2, pp. 1194-1201, April 2007

[24] N. Watson and J. Arrillaga, "Power Systems Electromagnetic Transients Simulation," London, U.K.: Inst. Elect. Eng., 2003

[25]R. P. Medeiros, F. Bezerra Costa, K. Melo Silva, J. d. J. C. Muro, J. R. L. Júnior and M. Popov, "A Clarke-Wavelet-Based Time-Domain Power Transformer Differential Protection," in IEEE Transactions on Power Delivery, vol. 37, no. 1, pp. 317-328, Feb. 2022

[26]M. Owen, "Transient analysis using component transforms," in PEAM 2011 - Proceedings: 2011 IEEE Power Engineering and Automation Conference, 2011, vol. 2, pp. 4–9.

[27]D. Bellan and G. Superti-Furga, "Three-phase transient analysis based on the space vector approach," TENCON 2017 - 2017 IEEE Region 10 Conference, 2017

[28]D. Bellan, "Transient Analysis of Single-Line-to-Ground Faults in Three-Phase Circuits Using Clarke Transformation," 2018 International Conference and Utility Exhibition on Green Energy for Sustainable Development (ICUE), 2018

[29]C. J. O'Rourke, M. M. Qasim, M. R. Overlin and J. L. Kirtley, "A Geometric Interpretation of Reference Frames and Transformations: dq0, Clarke, and Park," in IEEE Transactions on Energy Conversion, vol. 34, no. 4, pp. 2070-2083, Dec. 2019

[30] D. Bellan, "Transient Analysis of Single-Line-to-Ground Faults in Three-Phase Circuits Using Clarke Transformation," Proc. Conf. Ind. Commer. Use Energy, ICUE, vol. 2018-Octob, no. October, pp. 24–27, 2019.

[31]Bellan, D. "Clarke Transformation Solution of Asymmetrical Transients in Three-Phase Circuits," Energies 2020

[32]Rocha Junior, E.B.; Batista, O.E.; Simonetti, D.S.L. "Differential Analysis of Fault Currents in a Power Distribution Feeder Using abc, αβ0, and dq0 Reference Frames," Energies 2022

[33] P. J. Lagacé, L. A. Dessaint, M. Lavoie, J. Mahseredjian, and A. Chartrand, "Transient short circuit current calculation using decoupled networks," IEEE Trans. Power Deliv., vol. 14, no. 3, pp. 1110–1114, 1999.

[34] C. Concordia, "Relations Among Transformations Used in Electrical Engineering Problems," Gen. Electr. Rev., vol. 41, pp. 323–325, 1938.

[35] F. M. Gatta, A. Geri, S. Lauria, and M. Maccioni, "Analytical prediction of abnormal temporary overvoltages due to ground faults in MV networks," Electr. Power Syst. Res., vol. 77, no. 10, pp. 1305–1313, Aug. 2007.

[36] A. Cerretti, F. M. Gatta, A. Geri, S. Lauria, M. Maccioni, and G. Valtorta, "Ground fault temporary overvoltages in MV networks: Evaluation and experimental tests," IEEE Trans. Power Deliv., vol. 27, no. 3, pp. 1592–1600, 2012.

[37] A. Cerretti, F. M. Gatta, A. Geri, S. Lauria, M. Maccioni, and V. Valtorta, "Temporary overvoltages due to ground faults in MV networks," in 2009 IEEE Bucharest PowerTech: Innovative Ideas Toward the Electrical Grid of the Future, 2009.

[38] IEC TR 60071–4. (2004). "Insulation Co-ordination - Part 4: Computational Guide to Insulation Co-ordination and Modeling of Electrical Networks".

[39] Juan A. Martinez-Velasco, "Transient Analysis of Power Systems Solution Techniques, Tools and Applications", Wiley, 2015.

[40] A.I Ibrahim, "Frequency dependent network equivalents for electromagnetic transients studies: a bibliographical survey," International Journal of Electrical Power & Energy Systems, Volume 25, Issue 3, 2003.

[41] B. Gustavsen and A. Semlyen, "Rational approximation of frequency domain responses by vector fitting," in *IEEE Transactions on Power Delivery*, vol. 14, no. 3, pp. 1052-1061, July 1999, doi: 10.1109/61.772353.

[42]B. Gustavsen and H. M. J. De Silva, "Inclusion of Rational Models in an Electromagnetic Transients Program: Y-Parameters, Z-Parameters, S-Parameters, Transfer Functions," in IEEE Transactions on Power Delivery, vol. 28, no. 2, pp. 1164-1174, April 2013

[43] Gurunath Gurrala, Kiran Kumar Challa, “Comparison of vector and matrix format tangential interpolation for FDNE,” Electric Power Systems Research, Volume 197, 2021.

[44] “Alternate Transient Program (ATP) Rule Book,” Portl. OR Can. EMTP User Gr., 1995.